Magnetic Langmuir−Blodgett Films of Bimetallic Coordination Nanoparticles of $Cs_{0.4}Ni[Cr(CN)_6]_{0.9}$

Miguel Clemente-León,*[,†,‡] Eugenio Coronado,*[,†] Ángel López-Muñoz,[†] Diego Repetto,[†] Christophe Mingotaud,[⊥] Daniela Brinzei,[⊥] Laure Catala,*[,⊥] and Talal Mallah[⊥]

Instituto de Ciencia Molecular, Universidad de Valencia, Polígono de la Coma s/n, 46980 Paterna, Spain, Laboratoire des IMRCP-UMR 5623, Université Paul Sabatier, 118, Route de Narbonne, 31062 Toulouse cedex, France, and Institut de Chimie Moléculaire et des Matériaux d'Orsay, UMR CNRS 8182, Université Paris-Sud 11, 91405 Orsay, France

Received March 7, 2008. Revised Manuscript Received May 13, 2008

Magnetic Langmuir−Blodgett (LB) films of bimetallic coordination nanoparticles of the Prussian blue analogue $Cs_{0.4}Ni[Cr(CN)_6]_{0.9}$ were prepared by using the adsorption properties of a monolayer of dioctadecyldimethylammonium bromide (DODA). The molecular organization of the DODA monolayer is strongly affected by the presence of the water-dispersable $Cs_{0.4}Ni[Cr(CN)_6]_{0.9}$ nanoparticles in the subphase as has been shown by $\pi-A$ isotherms and Brewster angle microscopy (BAM) images at the air−water interface. BAM images suggest that a layer of inorganic nanoparticles is adsorbed under the monolayer of DODA, for high surface pressure and medium concentration of nanoparticles in the subphase and for all surface pressures at high concentrations of nanoparticles. Transfer of the monolayer onto different substrates allowed the preparation of multilayers containing $Cs_{0.4}Ni[Cr(CN)_6]_{0.9}$ nanoparticles. Magnetic properties of these LB films show a spin-glass-like behavior that can be explained by the strong magnetic dipolar interactions between the nanoparticles due to the small interparticle distances within the LB film. The magnetic properties of these LB films are very sensitive to the organization of the nanoparticles. They can be tuned by changing parameters such as the concentration of the subphase, the surface pressure, or the use of mixed monolayers. Thus, the Curie temperature of these LB films ranges from 60 K for the LB films prepared on the more concentrated subphase to 30 K for those prepared on the more diluted subphases. This is explained by the increase of interparticle distances and the subsequent weakening of the dipolar interactions between the nanoparticles within the LB film prepared on a subphase with a lower concentration of nanoparticles.

Introduction

Prussian blue analogues (PBA) have attracted great interest due to the large variety of magnetic properties they present that can be tuned either by magnetic field, light, temperature, or pressure. The magnetic properties of such 3-D coordination systems can be studied at the nanoscale in the form of nanoparticles. One of the main objectives of the preparation of coordination nanoparticles is on the one hand to study the effect of the size reduction on their cooperative magnetic properties and, on the other hand, to produce nanometric objects whose magnetic properties can be tuned by an external stimulus. Such particles may be potential candidates for single object information storage devices. Several methods have been reported in the literature to prepare PBA nanoparticles mainly using organic or inorganic protecting agents or templates.[1] Formation of charged particles is well-known for the PB soluble form and was described for the $Cu^{2+}/Fe(CN)_6^{3-}$ PBA analogue by Moulik et al., but with weak control on the size distribution.[1b] Use of hexametylphosphate counterions also recently was reported on $Ni/Fe(CN)_6^{3-}$ PBA to produce rather well-controlled 22 nm charged particles. Interestingly, electrostatic stabilization of

* Corresponding authors. E-mail: miguel.clemente@uv.es (M.C.-L.); eugenio.Coronado@uv.es (E.C.); and laurecatala@icmo.u-psud.fr (L.C.).
† Universidad de Valencia.
‡ Fundació General de la Universitat de València (FGUV).
⊥ Université Paul Sabatier.
§ Université Paris-Sud 11.

(1) (a) Dujardin, E.; Mann, S. *Adv. Mater.* **2004**, *16*, 1125. (b) Moulik, S. P.; De, G. C.; Panda, A. K.; Bhowmik, B. B.; Das, A. R. *Langmuir* **1999**, *15*, 8361. (c) Chow, P. Y.; Ding, J.; Wang, X. Z.; Chew, C. H.; Gan, L. M. *Phys. Status Solidi A* **2000**, *180*, 547. (d) Vaucher, S.; Li, M.; Mann, S. *Angew. Chem.* **2000**, *39*, 1793. (e) Vaucher, S.; Fielden, J.; Li, M.; Dujardin, E.; Mann, S. *Nano Lett.* **2002**, *2*, 225. (f) Catala, L.; Gacoin, T.; Boilot, J.-P.; Rivière, É.; Paulsen, C.; Lhotel, E.; Mallah, T. *Adv. Mater.* **2003**, *15*, 826. (g) Yamada-Sasano, M.; Arai, M.; Kurihara, M.; Sakamoto, M.; Miyake, M. *J. Am. Chem. Soc.* **2003**, *126*, 9482. (h) Arai, M.; Miyake, M.; Yamada, M. *J. Phys. Chem.* **2008**, *112*, 1953. (i) Uemura, T.; Kitawaga, S. *J. Am. Chem. Soc.* **2003**, *125*, 7814. (j) Uemura, T.; Ohba, M.; Kitagawa, S. *Inorg. Chem.* **2004**, *43*, 7339. (k) Uemura, T.; Kitawaga, S. *Chem. Lett.* **2005**, *34*, 132. (l) Catala, L.; Mathonière, C.; Gloter, A. O.; Stephan, T.; Gacoin, J.-P.; Boilot, T.; Mallah, T. *Chem. Commun. (Cambridge, U.K.)* **2005**, *6*, 746. (m) Kong, Q.; Chen, X. G.; Yao, J. L. *Nanotechnology* **2005**, *16*, 164. (n) Guari, Y.; Larionova, J.; Molvinger, K.; Folch, B.; Guerin, C. *Chem. Commun. (Cambridge, U.K.)* **2006**, 2613. (o) Brinzei, D.; Catala, L.; Mathoniere, C.; Wernsdorfer, W.; Gloter, A.; Stephan, O.; Mallah, T. *J. Am. Chem. Soc.* **2007**, *129*, 3778. (p) Dominguez-Vera, J. M.; Colacio, E. *Inorg. Chem.* **2003**, *42*, 6983. (q) Gálvez, N.; Sánchez, P.; Domínguez-Vera, J. M. *Dalton Trans.* **2005**, *15*, 2492. (r) Moore, J. G.; Lochner, E. J.; Ramsey, C.; Dalal, N. S.; Stiegman, A. E. *Angew. Chem., Int. Ed.* **2003**, *42*, 2741. (s) Clavel, G.; Guari, Y.; Larionova, J.; Guerin, C. *New J. Chem.* **2005**, *29*, 275. (t) Folch, B.; Guari, Y.; Larionova, J.; Luna, C.; Sangregorio, C.; Innocenti, C.; Caneschi, A.; Guerin, C. *New J. Chem.* **2008**, *32*, 273. (u) Zhou, P. H.; Xue, D. S.; Luo, H. Q.; Chen, X. G. *Nano Lett.* **2002**, *2*, 845. (v) Clavel, G.; Larionova, J.; Guari, Y.; Guérin., C. *Chem.—Eur. J.* **2006**, *12*, 3798. (w) Baioni, A. P.; Vidotti, M.; Fiorito, P. A.; Ponzio, E. A.; de Torresi, S. I. C. *Langmuir* **2007**, *23*, 6796.

10.1021/cm8006765 CCC: $40.75
Published on Web 06/21/2008

homogeneous 6 nm $Cs_{0.4}Ni[Cr(CN)_6]_{0.9}^{0.3-}$, $Cs_{0.4}Ni[Cr(CN)_6]_{0.9}$, nanoparticles without any added agent, was achieved by the combined effect of cesium insertion with an excess of hexacyanochromate.[2] This straightforward method enabled us to produce small, controlled particles that are single domain and that may be processed easily.

The development of processing techniques to organize these nanoparticles is indeed an important step for different possible applications (magnetic, photomagnetic, and electrochromic devices). An elegant approach to arrange molecules into well-organized multilayered films is the Langmuir−Blodgett (LB) technique.[3] This technique has been widely applied to create ultrathin films with a specific architecture that can be used as chemical sensors, modified electrodes, or molecular electronic devices.[4] It also can be used to prepare thin films of magnetic clusters or nanoparticles such as polyoxometalates,[5] Mn_{12} single-molecule nanomagnets,[6] iron oxide nanoparticles,[7] or the protein ferritin.[8] Several groups have reported the preparation of LB films of PBA nanoparticles. One of us was the first to prepare PB nanoparticles of the copper hexacyanoferrate analogue using the LB technique by the adsorption of negatively charged nanoparticles dissolved in water along a positively charged monolayer such as dioctadecyldimethylammonium bromide (DODA) or an amphiphilic Ru complex spread at the air−water interface. It was found that depending on the concentration of the precursors of the nanoparticles in the subphase, two different regimes could be found. For higher concentrations ($>10^{-5}$ M), PBA colloids were adsorbed in the interface by electrostatic interactions leading to rough multilayers, while well-organized multilayer LB films were obtained for more diluted solutions in which (partial) dissolution of the PBA colloids was observed.[9] Nanocubes with sizes ranging from 30 to 200 nm were reported to crystallize at the water−air interface for mixtures of $K_3M(CN)_6$ (M = Fe, Co, Cr) with $M'(ClO_4)_2$ (M' = Cu, Ni) with DODA as a cationic surfactant.[10] Bagkar et al. reported the use of LB films of 100 nm nickel hexacyanoferrate nanoparticles adsorbed on a DODA monolayer for potassium ion sensing.[11] Very recently, LB films of PBA nanoparticles of 20 nm were prepared by Ohnuki et al. using octadecyltrimethylammonium as the amphiphile.[12] These LB films were used as amperometric glucose biosensors. An alternative method was reported by Bagkar et al. for nickel hexacyanoferrate nanoparticles of ~22 nm. These LB films were prepared by extracting the nanoparticles from the aqueous solution with cetyltrimethylammonium bromide in $CHCl_3$ and spreading these surfactant encapsulated nanoparticles on pure water.[13]

In all these previous works of LB films of PBA nanoparticles, the particles have a magnetic behavior similar to that of the bulk because they are formed by several magnetic domains. This precludes any tuning of their magnetic response. Isolated 6 nm $Cs_{0.4}Ni[Cr(CN)_6]_{0.9}$ nanoparticles behave as single magnetic domains and were shown to be superparamagnetic with a blocking temperature below 10 K.[2] The LB technique can be a useful tool to control their organization and to tune their magnetic properties (blocking temperatures, coercive fields) by changing parameters such as the surfactant mixtures, the surface pressure, or the subphase concentration. This opens an interesting possibility to study a large variety of magnetic phenomena as compared to the LB films of larger particles. On the other hand, the use of such sub-10 nm nanoparticles may increase the density of magnetic information stored in these LB films that can be useful for magnetic storage devices. In this work, we studied the preparation and structural and magnetic characterization of LB films of 6 nm single-domain $Cs_{0.4}Ni[Cr(CN)_6]_{0.9}$ nanoparticles electrostatically stabilized in water that were then adsorbed onto a positively charged Langmuir monolayer of DODA.

Experimental Procedures

$Cs_{0.4}Ni[Cr(CN)_6]_{0.9}$ nanoparticles were prepared as reported in the literature.[2] An aqueous 2×10^{-3} M solution of $K_3Cr(CN)_6$ was added to an aqueous solution containing 2×10^{-3} M $NiCl_2 \cdot 6H_2O$ and 4×10^{-3} M CsCl. Different subphases were prepared by diluting the original solution of the nanoparticles to reach a final concentration of Ni^{2+} and $Cr(CN)_6^{3-}$ of 10^{-4}, 10^{-5}, 5×10^{-6}, and 10^{-6} M. In the following parts of the paper, concentrations of nanoparticles in the subphase will be given in equivalent Ni^{2+} and $Cr(CN)_6^{3-}$ concentrations. No problem of colloidal stability was observed for these solutions over a period of several hours, much longer than the length of the Langmuir experiments.

DODA dissolved in $CHCl_3$ was used as the spreading solution. An appropriate amount of this solution was carefully spread onto the aqueous subphase of the nanoparticles, and the spreading solvent was allowed to evaporate for 10 min prior to compression. The monolayer was compressed up to a surface pressure of 30 mN/m for transfer on the subphases of concentrations of 10^{-6} and 10^{-5} M, 40 mM/m on the 5×10^{-6} M subphase, and 15 mM/m on the 10^{-4} M subphase. Multilayer LB films were assembled to the substrates by the vertical lifting method (i.e., immersion and

(2) Brinzei, D.; Catala, L.; Louvain, N.; Rogez, G.; Stéphan, O.; Gloter, A.; Mallah, T. *J. Mater. Chem.* **2006**, *16*, 2593.
(3) Ulman, A. *An Introduction to Ultrathin Organic Films from Langmuir−Blodgett to Self-Assembly*; Academic Press: San Diego, 1991.
(4) Talham, D. R. *Chem. Rev.* **2004**, *104*, 5479.
(5) (a) Clemente-León, M.; Mingotaud, C.; Agricole, B.; Gómez-García, C. J.; Coronado, E.; Delhaes, P. *Angew. Chem., Int. Ed.* **1997**, *36*, 1114. (b) Clemente-Leon, M.; Agricole, B.; Mingotaud, C.; Gómez-García, C. J.; Coronado, E.; Delhaes, P. *Langmuir* **1997**, *13*, 2340. (c) Clemente-León, M.; Coronado, E.; Gómez-García, C. J.; Mingotaud, C.; Delhaès, P.; Ravaine, S.; Romualdo-Torres, G. *Chem.−Eur. J.* **2005**, *11*, 3979.
(6) Clemente-León, M.; Soyer, H.; Coronado, E.; Mingotaud, C.; Gómez-García, C. J.; Delhaès, P. *Angew. Chem., Int. Ed.* **1998**, *37*, 2842.
(7) (a) Iakovenko, S. A.; Trifonov, A. S.; Giersig, M.; Mamedov, A.; Nagesha, D. K.; Hanin, V. V.; Soldatov, E. C.; Kotov, N. A. *Adv. Mater.* **1999**, *11*, 388. (b) Fried, T.; Shemer, G.; Markovich, G. *Adv. Mater.* **2001**, *13*, 1158. (c) Telem-Shafir, T.; Markovich, G. *J. Chem. Phys.* **2005**, *123*, 204715.
(8) Clemente-León, M.; Coronado, E.; Soriano-Portillo, A.; Colacio, E.; Domínguez-Vera, J. M.; Gálvez, N.; Madueño, R.; Martín-Romero, M. T. *Langmuir* **2006**, *22*, 6993.
(9) Romualdo-Torres, G.; Agricole, B.; Mingotaud, C.; Ravaine, S.; Delhaès, P. *Langmuir* **2003**, *19*, 4688.
(10) Romualdo-Torres, G. Systèmes hybrides en films de Langmuir et Langmuir-Blodgett. Ph.D. Thesis, Université Bordeaux 1, 2002.
(11) Bagkar, N.; Betty, C. A.; Hassan, P. A.; Kahali, K.; Bellare, J. R.; Yakhmi, J. V. *Thin Solid Films* **2006**, *497*, 259.
(12) Ohnuki, H.; Saiki, T.; Kusakari, A.; Endo, H.; Ichihara, M.; Izumi, M. *Langmuir* **2007**, *23*, 4675.
(13) Bagkar, N.; Ganguly, R.; Choudhury, S.; Hassan, P. A.; Sawant, S.; Yakhmi, J. V. *J. Mater. Chem.* **2004**, *14*, 1430.

withdrawal of the substrate through the interface covered by the film). The modified slide after emersion was dried with air previously to the next immersion; otherwise the transfer ratio decreased in the successive dipping cycles. The dipping speed of the substrates was 1 cm/min. CaF_2 substrates coated with three monolayers of behenic acid if needed were used for infrared (IR) spectroscopy, hydrophilic glass substrates for atomic force microscopy (AFM), and mylar substrates for magnetic measurements.

Isotherms were obtained with a NIMA trough (type 601BAM) equipped with a Wilhelmy plate and maintained at 20 °C. A KSV3000 trough was used to prepare the LB films. Millipore water with a resistivity higher than 18 MΩ cm was used in all the experiments. A BAM2plus from NFT was used for the Brewster angle microscopy experiments.

Dynamic light scattering (DLS) experiments were performed on a Malvern nanozetasizer apparatus (equipped with a backscattering mode) on 1.5 mL of an aqueous solution. The volume profile was used to estimate the size corresponding to the main peaks keeping in mind that it underestimates the proportion of smaller particles. IR spectra were recorded on a FTIR 320 Nicolet spectrometer. UV−vis spectra were recorded on a Shimadzu UV-2401PC spectrometer. A commercial atomic force microscope (Multimode SPM by Veeco) was employed for surface sample characterization.

The magnetic measurements were performed with a Quantum Design MPMS-XL SQUID magnetometer. For those experiments, 29 monolayers were deposited onto a diamagnetic mylar sheet (0.075 mm × 5 mm × 15 mm). The procedure followed for the magnetic susceptibility is described elsewhere.[5a] The isothermal magnetization studies were performed at the same sweeping rate as the magnetic field for all samples.

Results and Discussion

We used a simple procedure described elsewhere to obtain the stabilization of $Cs_{0.4}Ni[Cr(CN)_6]_{0.9}$ nanoparticles in an aqueous subphase.[2] This method leads to the stabilization of charged particles with a size of 6 nm.

Preparation of a Layer of $Cs_{0.4}Ni[Cr(CN)_6]_{0.9}$ Nanoparticles. The first step to prepare LB multilayers of these nanoparticles was the preparation of a monolayer of DODA at the air−water interface. The negatively charged nanoparticles dissolved in the aqueous subphase were adsorbed onto this positively charged monolayer by electrostatic interactions. To find the best conditions for the LB transfer, we tried several concentrations of nanoparticles by diluting the original aqueous solution of nanoparticles. Since the concentration of $Cr(CN)_6^{3-}$ and Ni^{2+} in the original solution of nanoparticles was 10^{-3} M, we called the subphases 10^{-4}, 10^{-5}, 5×10^{-6}, and 10^{-6} M for nanoparticle solutions diluted 10, 100, 500, and 1000 times, respectively. DLS experiments confirmed that nanoparticles were preserved for the 10^{-3}, 10^{-4}, and 10^{-5} M subphases (hydrodynamical radius of ca. 8 nm), but no signal was observed for concentrations below 5×10^{-6} M. Either this technique was not sensitive enough for concentrations lower than 5×10^{-6} M or the particles fell apart for such low concentrations.

***π*−*A* Isotherms.** Figure 1 shows the isotherms corresponding to the DODA monolayer on a subphase in the absence and presence of nanoparticles at different concentrations. Several effects can be observed. For the more diluted concentrations (10^{-6}, 5×10^{-6}, and 10^{-5} M), the isotherm is shifted toward smaller areas per molecule as compared to a pure water subphase. This easily can be explained by the adsorption of ions along the interface that counterbalance the repulsion between the positively charged head groups of DODA. This effect also was observed for DODA with a large variety of charged anions.[5,9,14] For the 10^{-6} M subphase, the isotherm is very similar to that of DODA in a water subphase containing $K_3Cr(CN)_6$ at the same concentration (10^{-6} M) (see Supporting Information).[10] This could indicate the decomposition of the $Cs_{0.4}Ni[Cr(CN)_6]_{0.9}$ nanoparticles into their components (Ni^{2+}, Cs^+, and $[Cr(CN)_6]^{3-}$ ions). This effect was confirmed by BAM and by the IR spectra of the transferred film. When the concentration of the nanoparticles is increased, the isotherms are shifted toward higher areas per molecule. At the same time, changes in the collapse surface pressure also are observed. This behavior also was observed for concentrated solutions of other anionic species such as polyoxometalates.[15] In this case, when the concentration of polyanions exceeds a critical value C_c, corresponding to the highest density of the film, further addition of polyanions to the subphase leads to a re-expansion of the monolayer.[15] The explanation for this behavior is that at the critical concentration, C_c, the DODA monolayer becomes saturated. Hence, above C_c, the polyanions can be adsorbed only by formation of a diffuse double layer by means of small cations of the subphase. The thickening of the inorganic sublayer would weaken the interactions between polyanions and DODA monolayer and then lower the density of the latter at increasing concentrations of polyoxometalates.[16] The behavior of a DODA monolayer on a subphase containing $Cs_{0.4}Ni[Cr(CN)_6]_{0.9}$ nanoparticles could be explained by the same effect. The main difference with respect to the polyoxometalate solutions is that the shifts toward higher surface pressures are much more important for the nanoparticle solutions. This may be due to the larger size and higher charge of $Cs_{0.4}Ni[Cr(CN)_6]_{0.9}$ nanoparticles (ca. −600 per particle) with respect to the polyoxometalates. We took into account furthermore that other effects could complicate the interpretation of the isotherms such as the aggregation of the nanoparticles under the monolayer or their

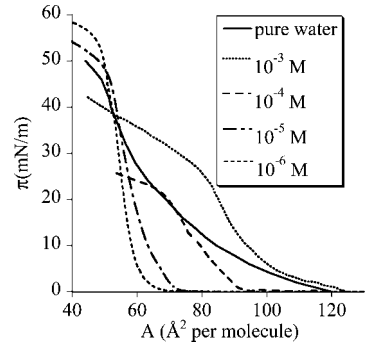

Figure 1. *π*−*A* isotherms of different DODA monolayers prepared at the air−water interface: pure water (solid line) and in presence of various concentrations of nanoparticles (see text).

(14) Aiai, M.; Ramos, J.; Mingotaud, C.; Amiell, J.; Delhaès, P.; Jaiswal, A.; Singh, R. A.; Singh, B.; Singh, B. P. *Chem. Mater.* **1998**, *10*, 728.
(15) Kahn, J. G.; Monroy, F.; Mingotaud, C. *Phys. Chem. Phys. Chem.* **2003**, *5*, 2648.
(16) Cuvillier, N.; Bernon, R.; Doux, J.-C.; Merzeau, P.; Mingotaud, C.; Delhaès, P. *Langmuir* **1998**, *14*, 5573.

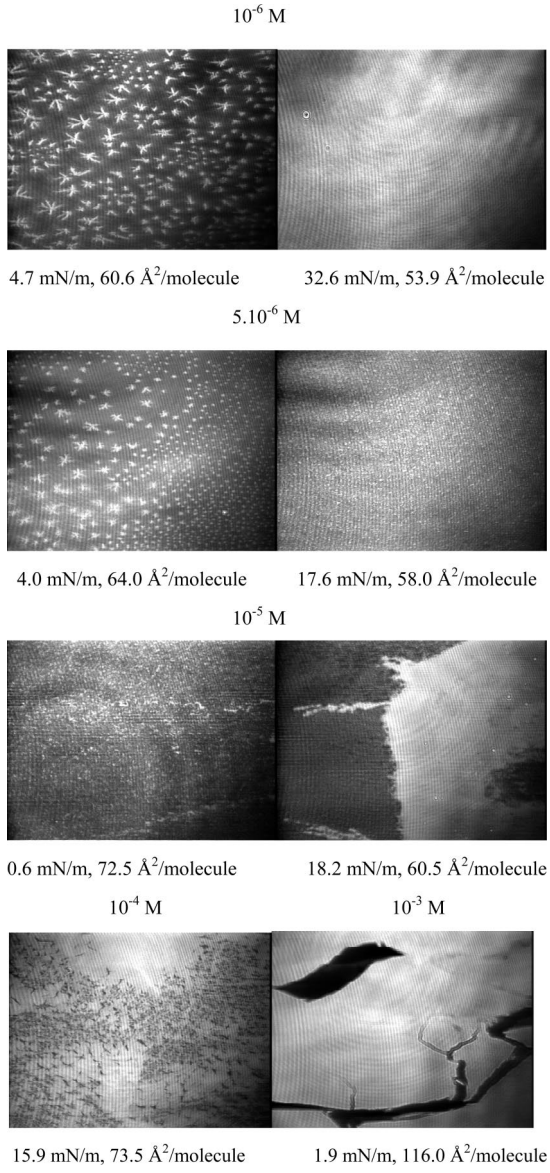

Figure 2. BAM images of a DODA monolayer, at the air−water interface, on different concentrations of nanoparticles in the subphase under different surface pressures. Real size: 430 μm × 536 μm. The intensity scale was adjusted for all images.

partial decomposition mentioned previously. On the other hand, the isotherm of DODA in a 10^{-4} M nanoparticle solution is very different from that of DODA in a 10^{-4} M $K_3Cr(CN)_6$ subphase (see Supporting Information). This is in line with the fact that at this concentration, the isotherm results from adsorption of nanoparticles present in solution as confirmed by the BAM images.

BAM. DODA monolayers in the presence of nanoparticles in the subphase were observed directly by BAM at the air−water interface to obtain information about the morphology of the different films. Typical images of a DODA monolayer on a 10^{-6} M subphase are shown in Figure 2. When the surface pressure is increased (see image at $\pi =$ 4.7 mN/m), bright and star-like domains appear on the uniform and gray background. This should correspond to a phase transition from a liquid expanded (gray domains) to a liquid condensed (white domains) phase. These white islands became more dense as the surface pressure was increased, leading at high surface pressure to a homogeneous monolayer as demonstrated by the uniformly bright BAM images recorded at those surface pressures (see image at $\pi = 32.6$ mN/m). Such a behavior was previously described for DODA on pure water and on a polyoxometalate subphase.[16] We can conclude, therefore, that the behavior of DODA on a 10^{-6} M subphase of nanoparticles is similar to that obtained for DODA on subphases containing inorganic ions, such as the polyoxometalates. When the concentration of nanoparticles is increased in the subphase, changes in the layer morphology are observed. For example, Figure 2 shows images of a DODA monolayer on a 5×10^{-6} M subphase. At the beginning of the compression, the behavior is similar to that observed on a 10^{-6} M subphase with bright star-like domains appearing and then fusing together (see image at $\pi = 4.0$ mN/m). But, for high surface pressures (see image at $\pi =$ 17.6 mN/m), an inhomogeneous phase with brighter points appears instead of the homogeneous phase obtained on the 10^{-6} M subphase. The reflectivity of the brighter points is much higher than that of the continuous liquid condensed phase observed on the 10^{-6} M subphase. On a 10^{-5} M subphase, the DODA monolayer shows from the beginning of compression the presence of brighter points of high reflectivity similar to those obtained on the 5×10^{-6} M subphase at high surface pressures (see image at 0.6 mN/m). At higher surface pressures, a very bright phase is formed that coexists with a less homogeneous phase of lower reflectivity (see image at 18.2 mN/m). Similar images were recorded on concentrated 10^{-4} and 10^{-3} M subphases (see images at 15.9 mN/m for the 10^{-4} M subphase and 1.9 mN/m for the 10^{-3} M subphase). The brightness of the layer observed by BAM could be explained by the large increase of interface thickness when nanoparticles of ca. 6 nm are adsorbed under the DODA layer.[15] Therefore, these images suggest that a layer of inorganic nanoparticles is adsorbed under the organic monolayer of DODA, for high surface pressure and medium concentration of nanoparticles in the subphase, and for all surface pressures at high concentrations of nanoparticles. On the other hand, the BAM images obtained on a 10^{-6} M subphase are consistent with the adsorption of simple anions under the DODA monolayer. This suggests again decomposition of the nanoparticles, the resulting $Cr(CN)_6^{3-}$ anions being adsorbed under the DODA film. This is in agreement with the compression isotherm and IR spectra of the transferred films.

Preparation of LB Films of $Cs_{0.4}Ni[Cr(CN)_6]_{0.9}$ Nanoparticles. An important aspect of the usefulness of the complex monolayer fabricated at the air−water interface is its subsequent transfer to a solid substrate. In the present work, we used the vertical lifting method to transfer monolayers of DODA at different concentrations of nanoparticles. Repeated dipping cycles allowed the preparation of LB multilayer films for four equivalent concentrations (i.e., 10^{-6}, 5×10^{-6}, 10^{-5}, and 10^{-4} M). On a 10^{-3} M subphase, it was not possible to prepare LB films having more than one monolayer of DODA. Y-type LB films (transfer on the dowstroke and upstroke of the substrate) with transfer ratios close to unity were obtained at a surface pressure of 30 mN/m for the subphases with a 10^{-5} and 10^{-6} M concentration

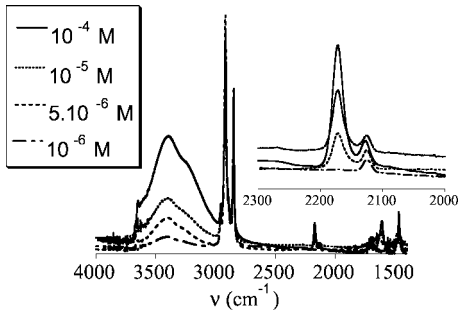

Figure 3. IR spectra of LB films prepared on 10^{-6} M (19 monolayers deposited on CaF_2), 5×10^{-6} M (20 monolayers deposited on CaF_2 with three monolayers of behenic acid), 10^{-5} M (19 monolayers deposited on CaF_2), and 10^{-4} M (20 monolayers deposited on CaF_2 with three monolayers of behenic acid) subphases.

and 40 mN/m for the subphase with a 5×10^{-6} M concentration. For LB films prepared on a subphase with a 10^{-4} M concentration, transfer was achieved at a surface pressure of 15 mN/m. In this case, Z-type LB films were obtained (transfer on the upstroke only).

IR Spectroscopy. The IR spectra of LB films of DODA on the four different subphases (19 monolayers deposited on CaF_2 coated with three monolayers of behenic acid if needed) are shown in Figure 3. All of them present bands at 2918, 2848, and 1470 cm^{-1} assigned to CH_2 stretching or scissoring vibrations of DODA (and eventually of the sublayers of behenic acid). The IR spectrum of powder samples of the $Cs_{0.4}Ni[Cr(CN)_6]_{0.9}$ nanoparticles reported in the literature shows a strong band at 2170 cm^{-1} that can be assigned to the elongation mode of bridging cyanide and a shoulder at ~2130 cm^{-1} assigned to free cyanides at the surface of the nanoparticles.[17] Large differences in these bands related to the cyanide ligands were found for the LB films. Whereas the LB film prepared on a 10^{-6} M subphase shows only one band at 2125 cm^{-1} (elongation of the nonbridging CN ligand), the LB films prepared on the 5×10^{-6}, 10^{-5}, and 10^{-4} M subphases present an additional band at higher wavelengths (bridging cyanide ligands). This fact supports the decomposition of nanoparticles in the 10^{-6} M subphase as already suggested by compression isotherms and BAM images since only free $Cr(CN)_6^{3-}$ anions were detected. The LB films obtained on 10^{-4}, 10^{-5}, and 5×10^{-6} M subphases present similar IR spectra with a strong band at 2173 cm^{-1} and a shoulder around 2126 cm^{-1}. Therefore, the IR spectra of the LB films prepared at these concentrations are consistent with the presence of nanoparticles. The relative intensity of the band assigned to bridging CN decreases with decreasing concentration. Since the 6 nm particles were found to be stable at 10^{-4} M by DLS, the decrease of bridging cyanides with respect to the nonbridging atoms when decreasing the particles' concentration indicates the presence of an equilibrium that favors the formation of free $Cr(CN)_6^{3-}$ species at concentrations lower or equal to 5×10^{-6} M.

Finally, the presence of water molecules was detected in the IR spectra of these LB films with bands centered at 3650, 3400, and 1610 cm^{-1}. These bands can be assigned to water molecules in the metal−cyanide network of the nanoparticles as in other LB films of PBA.[10] The intensity of these bands decreases with the concentration of the subphase in a similar way as the relative intensity of the band assigned to bridging CN. We carried out complete characterization of LB films obtained at 10^{-4}, 10^{-5}, and 5×10^{-6} M concentrations in which the presence of Ni−NC−Cr bands was detected.

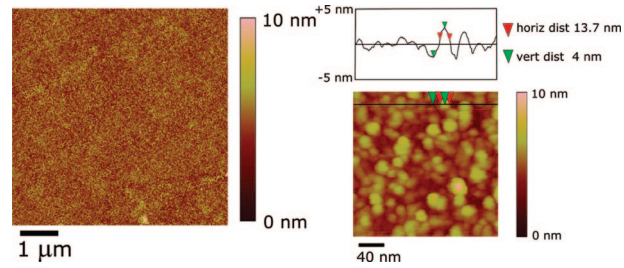

Figure 4. AFM image of a LB film of one monolayer deposited on glass prepared on a 10^{-5} M subphase.

AFM. The morphology of these LB films further was studied by AFM. For this purpose, samples from different subphases (10^{-4}, 10^{-5}, and 5×10^{-6} M) and of various thickness (1−19 monolayers) were prepared and transferred onto glass substrates. Figure 4 shows the typical topography of a LB film formed by one monolayer prepared on a 10^{-5} M subphase. The entire surface was covered homogeneously (root-mean-square (rms) roughness of ~1.1 nm) with (spherical) particles having an apparent diameter between 10 and 15 nm. The lateral resolution depends on the radius of the tip employed for the measurements, which is ~10 nm in our case. The features in the previous image come from convolution between tip and sample. Thus, the diameter of the particles is clearly overestimated.[18] Section analysis of the enlarged image shows that the maximum height differences are ~6 nm (Figure 4), a value close to the mean diameter of the nanoparticles as estimated in solution by DLS. Therefore, AFM measurements indicate that the nanoparticles are present in compact packing within the transferred monolayer. It seems that the morphology of the film is determined by the nanoparticles as they present a much larger size than the surfactant molecules also present in the LB film as shown by IR spectroscopy. In all the observed images, the whole surface is covered by nanoparticles. Flatter and lower zones that could correspond to the transfer of a monolayer of the surfactant without nanoparticles are not detected. Therefore, the DODA molecules may be placed around the nanoparticles by electrostatic interactions.

AFM images on LB films of 9 monolayers (Figure 5a) prepared on a 10^{-5} M subphase also show spherical particles with an apparent diameter of ~15 nm. The most important effect of the deposition of more monolayers is the increase in the height differences, which reach maximum values of ~20 nm. This may be explained by an imperfect layer-by-layer growth of the film because of incomplete coverage for each monolayer. Interestingly, the maximum height differences do not increase by adding another 10 monolayers to the film (Figure 5b). This indicates that the zones of lower height of the LB film are filled by the deposition of more

(17) Catala, L.; Gloter, A.; Stephan, O.; Rogez, G.; Mallah, T. *Chem. Commun. (Cambridge, U.K.).* **2006**, 1018.

(18) Schmitt, J.; Machtle, P.; Eck, D.; Mohwald, H.; Helm, C. A. *Langmuir* **1999**, *15*, 3256.

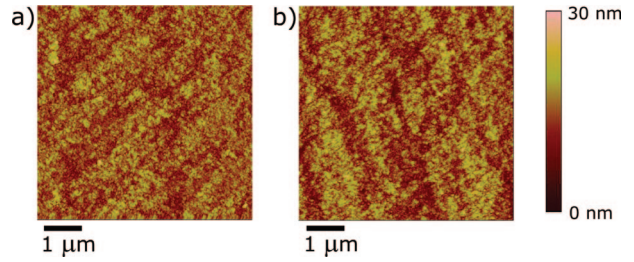

Figure 5. AFM image of LB films of 9 monolayers (a) and 19 monolayers (b) deposited on glass prepared on a 10^{-5} M subphase.

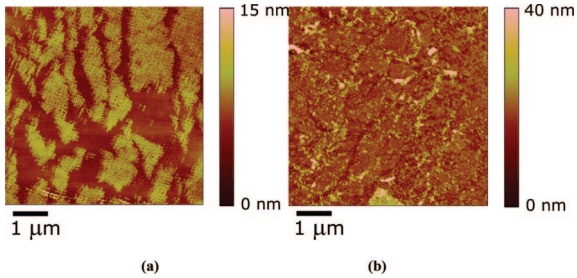

Figure 6. AFM image of LB films of 1 monolayer deposited on glass prepared on a 5×10^{-6} M subphase (a) and a 10^{-4} M subphase (b).

monolayers from the air−water interface. This is confirmed by a slight increase in the rms roughness, which is 3.1 and 3.6 nm for 9 and 19 monolayer films, respectively.

The concentration of the subphase plays a crucial role in the formation of a homogeneous LB film. By lowering it to 5×10^{-6} M, it is not possible to cover the whole substrate, and close packed nanoparticle islands of average height ∼6 nm and rms roughness ∼1 nm are formed (Figure 6a) for a LB film of one monolayer. These islands present the same morphology (i.e., homogeneous film) than the one on a 10^{-5} M subphase. Despite the lower homogeneity of the LB films with 1 monolayer, when 9 monolayers are deposited on this subphase, LB films exhibiting a similar morphology and same rms roughness values (i.e., 3 nm) to those prepared on a 10^{-5} M subphase are obtained. It seems that the lower zones of the LB film with 1 monolayer also are filled after the deposition of more monolayers. These lower and flatter regions in the LB film with 1 monolayer could correspond to the naked substrate or to zones of the substrate covered only by surfactant molecules. In this last case, the presence of free $Cr(CN)_6^{3-}$ anions in this lower and flatter zone could explain the increase of the relative intensity of the IR band assigned to nonbridging CN^- as compared to that of bridging compounds observed in these LB films.

An increase in the concentration of the subphase to 10^{-4} M leads to less homogeneous LB films. AFM images of LB films with 1 monolayer show an inhomogeneous surface in which areas of bare substrate, islands of close packed nanoparticles (∼6 and 12 nm in height), as well as aggregates of heights up to 30 nm are all present (Figure 6b). This result suggests either the presence of multilayers or that of larger particles due to the aggregation of 6 nm nanoparticles while forming the film.

To summarize, we have shown that the morphologies of the LB films are strongly dependent on the concentration of the subphase: When depositing a single layer, using a subphase of 10^{-4} M, particles of 6 nm tend to aggregate in some regions, and a very close packing in the film is observed, while a 10^{-5} M subphase leads to a uniform film of 6 nm particles. The intermediate concentration of 5×10^{-6} M gives a less compact film with regions probably containing hexacyanochromate ions. When depositing more layers, these regions are filled by particles and a similar roughness is obtained for the 10^{-5} and 5.10^{-6} M subphases.

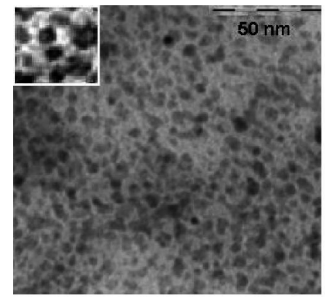

Figure 7. TEM image of a LB film of 1 monolayer deposited on Cu grids coated with Formvar prepared on a 10^{-4} M subphase.

Transmission Electronic Microscopy (TEM). For direct observation of the nanoparticles on the transferred LB films, TEM experiments were carried out on LB films with 1 monolayer transferred on Cu grids coated with Formvar. Figure 7 shows a TEM image of a LB film of one monolayer prepared on the 10^{-4} M subphase. The entire surface is covered with nanoparticles with a size between 5 and 8 nm, proving that the nanoparticles present in solution were adsorbed along the DODA monolayers and then transferred onto the substrate during LB film formation. The nanoparticles are isolated and uniformly distributed along the observed surface. This result suggests that the aggregates of heights up to 30 nm observed by AFM are due to the presence of multilayers. The presence of larger particles due to aggregation is excluded as they are not observed by TEM.

Magnetic Properties. The magnetic properties of this type of nanoparticles in the powder form already were studied.[2] They show either a superparamagnetic or a spin-glass-like behavior depending on the isolation technique used. Nanoparticles coated with a great excess of polymer and recovered from solution show a superparamagnetic behavior with a blocking temperature of 9 K.[2] When the interparticle distances are decreased, as occurs in samples coated with a low content of polymer or with a surfactant, strong interactions occur, leading to a spin-glass-like behavior.[2]

Magnetic properties of LB films of $Cs_{0.4}Ni[Cr(CN)_6]_{0.9}$ nanoparticles were measured. Thirty monolayers of these LB films were deposited onto a diamagnetic mylar substrate. Contrary to other LB films of magnetic clusters or nanoparticles,[5,6,8] a small number of monolayers (usually less than 30) is enough to obtain a magnetic response recordable on a SQUID magnetometer. Furthermore, out-of-phase ac signals can be measured, which is not possible in many other magnetic LB films. This is probably a consequence of the single-domain effect that leads to superparamagnetic behavior and thus to a relatively large magnetic signal, everything being equal.

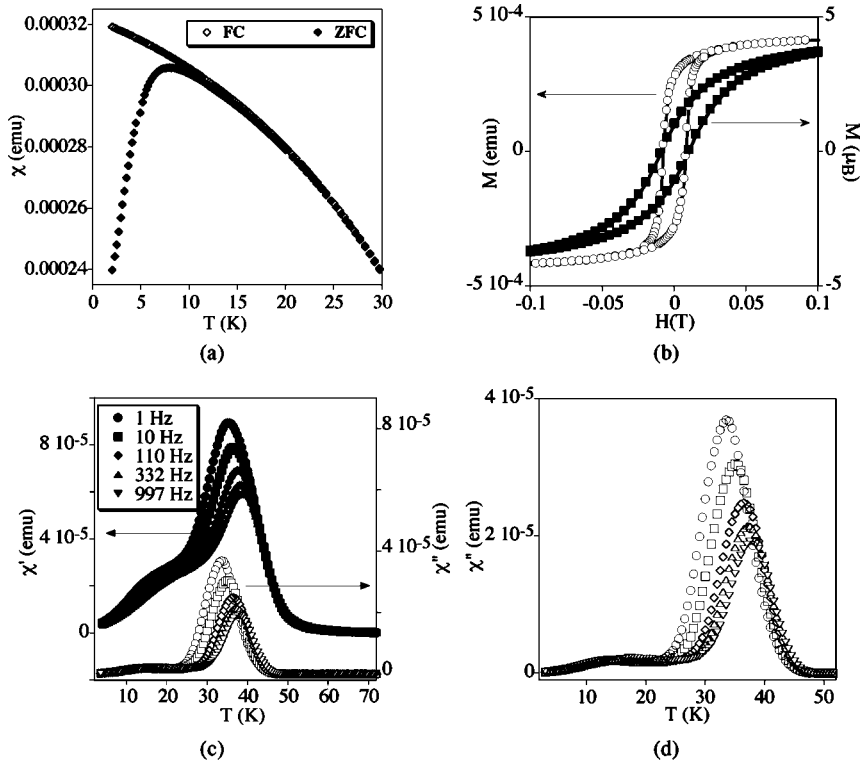

Figure 8. Magnetic properties of a LB film prepared on a 10^{-5} M subphase. Thermal dependence of the ZFC and FC susceptibility with an applied field of 50 G (a); hysteresis loop of magnetization of a powder sample of nanoparticles diluted into a polymer matrix (solid squares) and a LB film (open circles) (at 2 K) (b); temperature dependence of the in-phase ac susceptibility (χ) (solid symbols) and out-of-phase ac susceptibility (χ'') (open symbols) (c); and temperature dependence of the out-of-phase ac susceptibility (χ'') (d).

The magnetic properties of the LB film prepared on a 10^{-5} M subphase are shown in Figure 8. Temperature dependence of the product of the magnetic susceptibility times temperature (not shown) exhibited an increase upon cooling, as expected for ferromagnetic exchange coupling between Ni(II) and Cr(III) bridged through cyanide. To characterize the behavior of the nanoparticles in this LB film, zero field cooled (ZFC) and field cooled (FC) magnetization measurements were carried out. The ZFC curve presents a maximum of the magnetization around 8 K, while ZFC and FC curves are superimposed above 15 K. This is a first indication of the blocking temperature (if the nanoparticles are single domain) or the Curie temperature (if they are in the multidomain regime). This behavior is very close to that found for powder samples, yet with a larger difference between the temperature of the maximum of the ZFC curve and the temperature where ZFC and FC gather.[2] This could indicate a stronger distribution of interparticle distances within the film as compared to the powder sample of nanoparticles homogeneously coated with a surfactant.[2] A marked hysteresis loop of magnetization was obtained with a coercive field of 80 G (Figure 8) at 2 K, which is similar to that observed on the powder sample. However, the hysteresis curve presents a very sharp increase of the magnetization at low fields (that saturates at 500 G) different from the S-shape observed on the powder samples of these nanoparticles diluted into a polymer matrix. Reduced magnetizations of 0.63 and 0.27 were, respectively, obtained for the LB film and the powder of randomly distributed particles.[2] Hence, organizing the particles in LB films strongly affects the shape of the hysteresis loop. To clarify the presence of interparticle interactions, ac magnetization measurements were carried out. The in-phase signal (χ') presents a maximum that is strongly frequency dependent with a shoulder at lower temperatures. The out-of-phase signal (χ'') begins to appear at 45 K (Figure 8) and presents a maximum shifted toward higher temperatures at increasing frequencies. This peak appears at higher temperatures than observed for diluted solutions of nanoparticles.[2] The frequency dependence of the maxima of the χ'' peaks can be fitted to an Arrhenius equation, $\ln(1/f) = \ln(\tau_0) + E_a/(KT)$, where f is the measuring frequency, τ_0 is the relaxation time, and E_a is the activation energy. However, the value of τ_0 obtained from this fitting ($\tau_0 = 10^{-28}$ s) does not lie in the range of values generally found for superparamagnetic particles (10^{-8} to 10^{-12} s). Much lower values without physical meaning as that obtained in this LB film were found for spin-glass behavior. Further evidence of this behavior is found from the ϕ parameter ($\phi = (T_{max} - T_{min})/(T_{max}(\log f_{max} - \log f_{min}))$, where T_{max} and T_{min} are temperatures corresponding to the maxima of the χ'' curves measured at the highest, f_{max}, and lowest, f_{min}, frequencies). In our LB film a value of $\phi = 0.036$ was obtained, which is lower than 0.1 found for isolated superparamagnetic nanoparticles.[19] Therefore, the LB film built on a 10^{-5} M subphase of nanoparticles presents spin-glass-like behavior that can be explained by the strong dipolar interactions between nanoparticles. This is in agreement with AFM images that show close contacts between the nanoparticles within the LB film.

(19) Vestal, C. R.; Song, Q.; Zhang, Z. J. *J. Phys. Chem. B* **2004**, *108*, 18222.

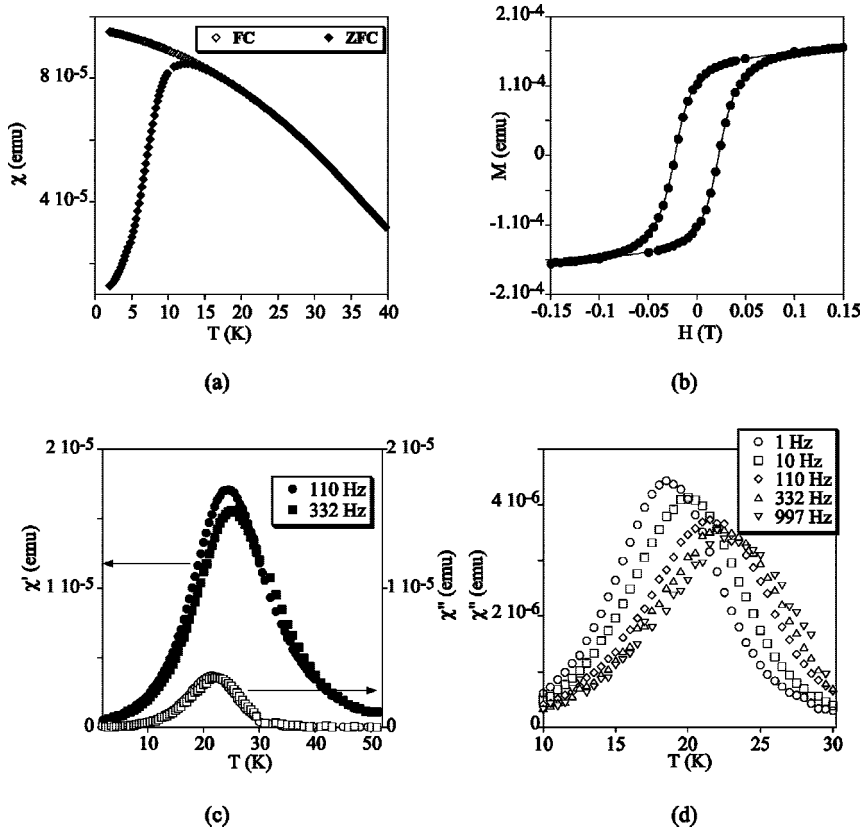

Figure 9. Magnetic properties of a LB film prepared on a 5×10^{-6} M subphase. Thermal dependence of the ZFC and FC susceptibility with an applied field of 50 G (a); hysteresis loop of magnetization at 2 K (b); temperature dependence of in-phase ac susceptibility (χ) (solid symbols) and out-of-phase ac susceptibility (χ'') (open symbols) (c); and temperature dependence of the out-of-phase ac susceptibility (χ'') (d).

The same effect was observed for powder samples of these nanoparticles coated with a surfactant or in aggregates embedded in a polymer that also present spin-glass-like behavior.[2] Moreover, the ac data show the presence of an in-phase and an out-of-phase secondary weak maxima around 15 K. The large difference in the temperature of the two peaks cannot be due to the presence of large and small particles but rather to the presence of relatively more isolated particles within the LB film that could be the cause of this secondary peak at lower temperatures. This supports the rather large difference between the maximum of the ZFC curve and the temperature where FC and ZFC curves coincide.

On the other hand, the representation of χ' versus χ'' at 35 K in the Cole−Cole plot (see Supporting Information) confirms that there is not a single relaxation process as would be expected for ideal superparamagnetic behavior. Thus, the fitting to the Debye model is far from an ideal semicircle and gives an α value close to 0.25 ($\alpha = 0$ for an infinitely narrow distribution of relaxation times).

Magnetic properties of a LB film prepared on a 5×10^{-6} M subphase are shown in Figure 9. The temperature and isothermal field dependence of magnetization are similar to those of the LB film prepared on a 10^{-5} M subphase and are indicative of the presence of ferromagnetic interactions. The temperature of the maximum of the ZFC curve (12 K) and the fact that the FC and ZFC curves are superimposed at 16 K, much closer to the maximum of the ZFC curve, may indicate a more homogeneous distribution of interparticle distances. The coercive field of the magnetization (220 G) is larger than that observed in the film prepared on the 10^{-5} M subphase, with a reduced magnetization of 0.57. The changes on the ac magnetization measurements are much clearer. A strongly frequency dependent χ' peak is observed. The maximum was found at a lower temperature as compared to the LB film built on a 10^{-5} M subphase. A χ'' peak also was observed below 32 K (Figure 9 and Supporting Information) and presents a maximum that is shifted toward higher temperatures at increasing frequencies. Again, the temperature of the maximum was found at lower temperatures as compared to the behavior of the LB film prepared on a more concentrated subphase. The ac peaks on the LB film prepared on a 5×10^{-6} M subphase are similar to the shoulder that appears at lower temperatures on the ac measurements of the LB film prepared on a 10^{-5} M subphase. The frequency dependence of the maxima of these χ'' peaks can be fitted to an Arrhenius equation, $\ln(1/f) = \ln(\tau_0) + E_a/(KT)$. The value of τ_0 obtained from this fitting ($\tau_0 = 4 \times 10^{-17}$ s) is much higher than that obtained for a LB film prepared on a 10^{-5} M subphase, but it still does not lie in the range of values generally found for superparamagnetic particles (10^{-8} to 10^{-12} s). Furthermore, the value of the ϕ parameter (0.065) is still lower than the 0.1 value generally found for isolated superparamagnetic nanoparticles.[19] Therefore, the magnetic properties of the LB film obtained on a 5×10^{-6} M subphase indicate a spin-glass-like behavior, but they are much closer to a superparamagnetic behavior of isolated nanoparticles. This could indicate that the dipolar interactions between the nanoparticles are decreased in the LB film prepared on a more diluted subphase due to the increase in the interparticle

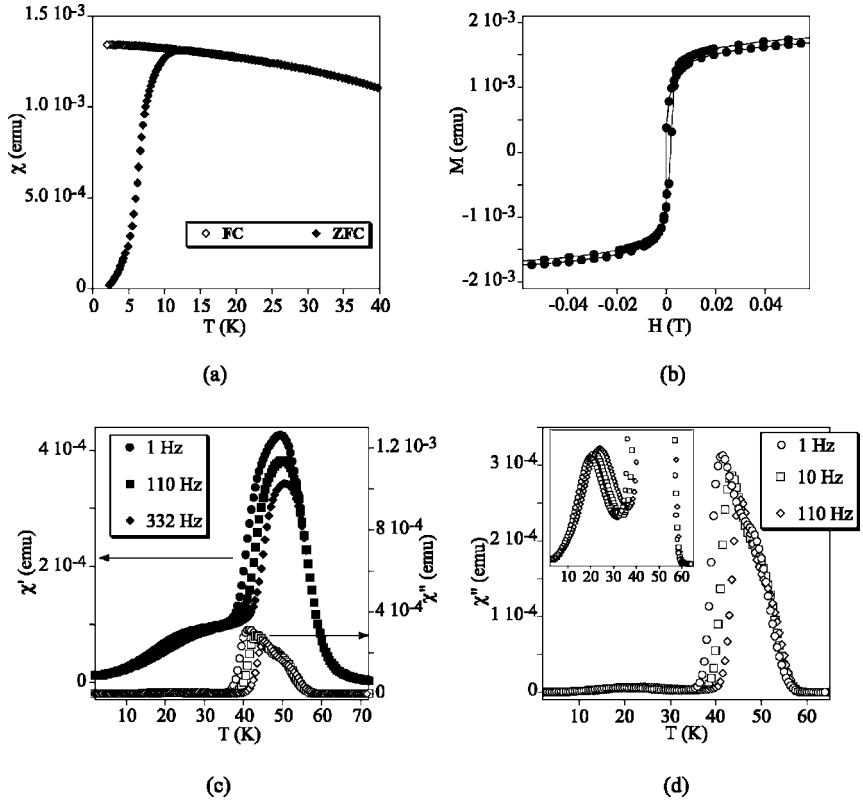

Figure 10. Magnetic properties of a LB film prepared on a 10^{-4} M subphase. Thermal dependence of the ZFC and FC susceptibility with an applied field of 50 G (a); hysteresis loop of magnetization at 2 K (b); temperature dependence of the in-phase ac susceptibility (χ) (solid symbols) and out-of-phase ac susceptibility (χ'') (open symbols) (c); and temperature dependence of the out-of-phase ac susceptibility (χ'') (d).

distances. This behavior also could be related to a change of size of the nanoparticles on the more diluted subphase, but this is excluded since AFM images show the same type of nanoparticles on the LB films prepared on the two subphases. It is hence possible to tune the dipolar interactions between the nanoparticles within the LB films by changing the concentration of the subphase.

The opposite effect was observed on a LB film with 30 monolayers prepared on a 10^{-4} M subphase. The square-shaped hysteresis still was observed but with a suppression of the coercive field. This already was observed when dipolar interactions largely increased in strength.[2] The ac measurements show peaks that are shifted to higher temperatures with respect to the LB film prepared on a 10^{-5} M subphase. Thus, the χ'' peaks begin to appear below 60 K (Figure 10), and they present a frequency dependent maximum with a shoulder at higher temperatures (ca. 50 K). At lower temperatures (below 30 K), there is a second and weaker peak that is also frequency dependent. The presence of the high temperature peak may be explained by the presence of large aggregates of connected particles induced by film formation, as observed by AFM measurements. The behavior of this LB film is still different from that of the bulk that presents much higher ordering temperatures (90 K). This result is not unexpected as a larger number of metal ions is located at the surface of nanoparticles as compared to the bulk, inducing a weaker Curie temperature (smaller number of neighboring atoms).

These results show that the χ'' peaks are shifted toward lower temperatures at decreasing concentrations due probably to a weakening of the dipolar interactions between the nanoparticles on the transferred films when the concentration is decreased. Conversely, the coercive fields of the LB films are stronger when the interparticle interactions are weakened. Another possible explanation for this behavior is a size dependence of nanoparticles with the concentration. The presence of larger particles on the LB film prepared on a 10^{-4} M subphase is not excluded, as shown by AFM images, whereas AFM images of LB films prepared on 10^{-5} and 5×10^{-6} M subphases show nanoparticles of similar size. To elucidate the effect of dipolar interactions between nanoparticles on the magnetic properties and to exclude size effects, two different strategies were developed in LB films prepared on the same subphase (10^{-5} M). The idea is to control the amount of adsorbed nanoparticles by changing the density of positively charged molecules on the Langmuir monolayer. Thus, a decrease of the concentration of the nanoparticles within the LB film should lead to an average increase of interparticle distances and hence to a decrease of dipolar interactions. These two strategies are (i) deposition at lower surface pressures (10 mN/m instead of 30 mN/m) and larger areas per molecule of surfactant and (ii) mixing the cationic DODA surfactant with a negatively charged surfactant such as DHP (dihexadecylphosphate) to separate the nanoparticles. In other anionic species such as polyoxometalates, it was found that the amount of adsorbed anions can be controlled by changing the ratio of these two surfactants. Thus, an excess of DHP causes no adsorption of the anion along the mixed monolayer, while an excess of the positively charged DODA causes adsorption of polyoxometalates, which is

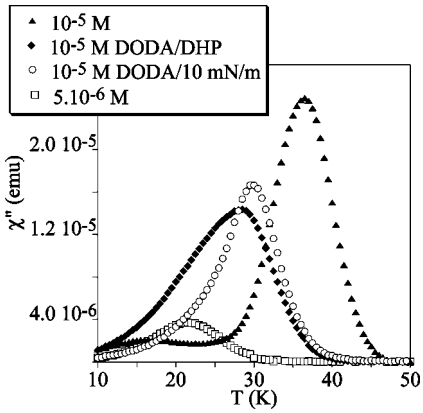

Figure 11. Temperature dependence of the out-of-phase signal (χ'') at 110 Hz of LB films of 30 monolayers prepared on a 10^{-5} M subphase with DODA at 30 mN/m (black triangles), with DODA at 10 mN/m (white circles), with a 1.1:1 DODA/DHP mixed monolayer at 30 mN/m (black rhombuses), and on a 5×10^{-6} M subphase with DODA at 40 mN/m (open squares).

a maximum in the absence of DHP.[5b] In the case of $Cs_{0.4}Ni[Cr(CN)_6]_{0.9}$ nanoparticles, both strategies led to Y-type LB films, although the transfer ratio decreased to a value close to 0.5 for the downstroke of the substrate in the LB film prepared at 10 mN/m. The magnetic properties of LB films of 30 monolayers obtained following these two strategies were measured. The temperature of the maximum of the ZFC curve is 15 K for that obtained at 10 mN/m and 13 K for that obtained at 30 mN/m on a 1.1:1 DODA/DHP mixed monolayer. Both LB films present a marked hysteresis loop in the magnetization, with a coercive field of 340 G for that obtained at 10 mN/m and 210 G for that obtained at 30 mN/m on a 1.1:1 DODA/DHP mixed monolayer. Out-of-phase ac magnetic properties at a given frequency (110 Hz) of the two LB films are shown in Figure 11. The temperature dependence of χ' and χ'' at different frequencies is shown as Supporting Information. The temperatures at which the χ'' peak becomes nonzero were decreased by ca. 7 K on the 1.1:1 DODA/DHP LB film ($\tau_0 = 2 \times 10^{-17}$ s and $\phi = 0.058$) with respect to that of the LB film prepared on pure DODA at 30 mN/m, but they are 10 K higher than those of the LB film prepared with pure DODA on a 5×10^{-6} M subphase. The same effect was observed for the LB film prepared at 10 mN/m ($\tau_0 = 5 \times 10^{-18}$ s and $\phi = 0.060$). Furthermore, the preparation of LB films with a larger excess of the positively charged surfactant, DODA, with respect to DHP, shifted the χ'' peak to higher temperatures. These peaks are always lower than those of the LB film of pure DODA.

These results indicate that both LB films present a spin-glass-like behavior with dipolar interactions between the nanoparticles weaker than in the LB film of pure DODA transferred at 30 mN/m. Therefore, both strategies were successful to tune the magnetic properties of the LB films of these nanoparticles. The χ'' peak of the LB film prepared on a 1.1:1 DODA/DHP mixed monolayer appears at slightly lower temperatures, and it is broader than that of the LB film prepared at 10 mN/m. This could indicate that dilution of DODA surfactant with DHP gives rise to slightly weaker dipolar interactions as compared to LB films prepared with pure DODA at 10 mN/m but to a less homogeneous distribution of interparticle distances within the film.

Finally, another possible strategy to weaken the dipolar interactions is to prepare the LB films on a subphase containing two types of PBA nanoparticles. For instance, the superparamagnetic $Cs_{0.4}Ni[Cr(CN)_6]_{0.9}$ nanoparticles could be diluted in the aqueous subphase with an excess of other diamagnetic or paramagnetic PBA nanoparticles. This would increase the distances between the $Cs_{0.4}Ni[Cr(CN)_6]_{0.9}$ nanoparticles within the LB film and could lead to LB films in which the superparamagnetic behavior of $Cs_{0.4}Ni[Cr(CN)_6]_{0.9}$ nanoparticles is preserved. This work is in progress.

Conclusion

We demonstrated that it is possible to organize in Langmuir monolayers and LB multilayers $Cs_{0.4}Ni[Cr(CN)_6]_{0.9}$ nanoparticles of ca. 6 nm by using adsorption of the negatively charged nanoparticles dissolved in the subphase onto a positively charged DODA monolayer spread at the air−water interface. Compression isotherms and BAM images obtained at different concentrations of nanoparticles revealed the formation of a thick layer of nanoparticles under the DODA monolayer for a high surface pressure and medium concentration of nanoparticles in the subphases (5×10^{-6} and 10^{-5} M) and for all surface pressures at high concentrations of nanoparticles (10^{-3} and 10^{-4} M). IR spectra of the transferred LB films indicated that the nanoparticles are present within the LB films prepared on 10^{-4}, 10^{-5}, and 5.10^{-6} M subphases. AFM measurements indicated that a homogeneous distribution of the nanoparticles was obtained for LB films prepared on a 10^{-5} M subphase. Magnetic properties of these LB films change drastically depending on the preparation conditions. LB films prepared on a 10^{-5} M subphase show a spin-glass-like behavior that can be explained by strong magnetic dipolar interactions between the nanoparticles due to the small interparticle distances within the LB film. The LB films prepared on a 5×10^{-6} M subphase present also a spin-glass-like behavior with smaller magnetic dipolar interactions. The interest of this method is that it permits the preparation of 2-D arrays of these nanoparticles that can be assembled into multilayer films with a very precise control of the thickness. The use of nanoparticles of such a small size opens the way for tuning magnetic properties by controlling their organization within the film, changing the preparation conditions and parameters such as the concentration of the subphase, the surface pressure, or the use of a mixture of surfactants. This method could be applied to other PBA nanoparticles presenting interesting magnetic properties such as photomagnetism or spin-crossover. Another interesting possibility may be the use of other electroactive surfactants providing a second property of interest that

can give rise to multifunctional films, as already was achieved with larger PBA nanoparticles.[9,20]

Acknowledgment. Financial support from the European Union (NoE MAGMANet, MERG-CT-2004-508033, and QUEMOLNA MRTN-CT-2003-504880), the Spanish Ministerio de Educación y Ciencia (Project Consolider-Ingenio in Molecular Nanoscience CSD2007-00010 and Projects CTQ2005-09385-C03 and MAT2007-61584), and the Generalitat Valenciana is gratefully acknowledged.

Supporting Information Available: Additional figures (PDF). This material is available free of charge via the Internet at http://pubs.acs.org.

CM8006765

(20) Romualdo-Torres, G.; Dupart, E.; Mingotaud, C.; Ravaine, S. *J. Phys. Chem. B* **2000**, *104*, 9847.